Inactivation of the Sodium Channel

II. Gating Current Experiments

CLAY M. ARMSTRONG and FRANCISCO BEZANILLA

From the Department of Physiology, University of Pennsylvania, School of Medicine, Philadelphia, Pennsylvania 19174

ABSTRACT Gating current (I_g) has been studied in relation to inactivation of the Na channels. No component of I_g has the time course of inactivation; apparently little or no charge movement is associated with this step. Inactivation nonetheless affects I_g by immobilizing about two-thirds of gating charge. Immobilization can be followed by measuring *ON* charge movement during a pulse and comparing it to *OFF* charge after the pulse. The *OFF:ON* ratio is near 1 for a pulse so short that no inactivation occurs, and the ratio drops to about one-third with a time course that parallels inactivation. Other correlations between inactivation and immobilization are that: (*a*) they have the same voltage dependence; (*b*) charge movement recovers with the time course of recovery from inactivation. We interpret this to mean that the immobilized charge returns slowly to "*off*" position with the time course of recovery from inactivation, and that the small current generated is lost in base-line noise. At −150 mV recovery is very rapid, and the immobilized charge forms a distinct slow component of current as it returns to *off* position. After destruction of inactivation by pronase, there is no immobilization of charge. A model is presented in which inactivation gains its voltage dependence by coupling to the activation gate.

INTRODUCTION

The experiments on sodium current reported in the preceding paper suggest that the activation gate of an Na channel must open before inactivation can occur. This suggestion is confirmed in this paper which describes the effects of inactivation on gating current (I_g). I_g is a small, relatively slow component of capacitative current, caused by the molecular rearrangements that open and close the ionic channels (Armstrong and Bezanilla, 1974; Keynes and Rojas, 1974; Meves, 1974). In theory, any voltage-dependent gating process must generate gating current, and there are three such factors in the Hodgkin and Huxley equations: m, which is related to activation of the Na channels; h, related to inactivation; and n, related to K activation (Hodgkin and Huxley, 1952*b*). h and n have slow kinetics and might be expected to generate gating currents of small amplitude. I_g associated with K activation has not yet been reported, although a suggestion of such a current is described below. We have searched for gating current associated with inactivation and have failed to find it, even under circumstances where it should probably be detectable if it

behaves as predicted by the Hodgkin and Huxley equations. On the other hand inactivation does affect I_g, for in inactivated membrane approximately two-thirds of gating charge is apparently immobilized by inactivation (Bezanilla and Armstrong, 1974; 1975*a*, *b*; Armstrong and Bezanilla, 1975). Several experiments are presented here to show that inactivation and gating charge immobilization are closely related and in fact are manifestations of the same process. These phenomena are explained by the same model presented briefly in the preceding paper. In terms of this model, inactivation gains its apparent voltage dependence from coupling to the activation process or, more explicitly, from the necessity for the activation gate of a sodium channel to open before its inactivation gate can close.

Two preliminary reports of this work have appeared elsewhere (Bezanilla and Armstrong, 1975*c*; Armstrong and Bezanilla, 1976). Similar results have recently been reported by Meves and Vogel (1977).

MATERIALS AND METHODS

All experiments were performed on giant axons from the squid *Loligo pealei*. Most of the procedures have been described in Materials and Methods of the preceding paper.

To allow comparison of the properties of I_{Na} and I_g, many experiments were performed in solutions containing a low concentration of Na^+ ion, so that the two currents were similar in magnitude. Tetrodotoxin (TTX) was usually added later in the experiment to allow determination of I_g alone, and I_{Na} was then found by subtracting I_g from the pre-TTX record.

Base lines for integration were flat lines fitted by eye to the segment of the trace between approximately 2.5 and 3.5 ms after the step. Unless noted, integration was over an interval of approximately 2.5 ms beginning with the step.

Solutions

The composition of the solutions used is listed in Table I. Measurements of membrane voltage have not been corrected for liquid junction potentials.

RESULTS

When Na Channels Open, No Component of I_g Has a Time Course Similar to Inactivation

Inactivation of the sodium channels is described in the Hodgkin and Huxley equations as a voltage-dependent process, and as such should have an associated gating current. We have searched for this current and have not been able to detect it. A typical experiment is illustrated in Fig. 1*a*, where I_{Na} and I_g are from an axon depolarized suddenly to +20 mV. I_g, the upper trace, has a brief rising phase followed by a falling phase that has at least two components (cf. Bezanilla and Armstrong, 1975*a*, *b*; Armstrong and Bezanilla, 1975). The slower component (called the slow *ON* component in what follows) is made evident by fitting an exponential to the trace between the points marked by arrows: the exponential, which is the smooth curve, clearly diverges from the experimental trace after the second arrow.

The slow *ON* component immediately suggests itself as Na inactivation or K activation gating current, but close examination shows that this cannot be the

case. First, the time constant of the slow *ON* component (τ_s^{ON}) and the decay time constant of I_{Na} (τ_h) are not equal (see Table II A). At positive voltages τ_h is consistently two or three times larger than τ_s^{ON}. Second, as illustrated in Fig. 1*b*, the slow *ON* component is not much affected by pronase, which destroys Na

TABLE I
COMPOSITION OF SOLUTIONS

	External solutions (mM)				
Name	Na	Tris*	Ca	Mg	Cl
ASW	440	5	10	50	570
5% NaSW	22	423	10	50	565
15% NaSW	66	369	10	50	555
20% NaSW	88	350	10	50	558
Tris SW		445	10	50	565
40 Na 50 Ca Tris	40	447	50		587
60 Na 50 Ca Tris	60	425	50		585
90 Na 50 Ca 40 Mg	90	310	50	40	580
	Internal solutions‡ (mM)				
Name	Na	TMA§	Cs	F	Glutamate
125 TMA		125		50	75
200 TMA		200		100	100
190 TMA 10 Na	10	190		75	125
125 Cs		125		125	
447 Cs			447	447	

* Tris (hydroxymethyl) aminomethane.
‡ Sucrose was added to adjust osmolality to 980 mosmol/kg. 1 mM HEPES or 5 mM Tris was used as buffer.
§ Tetramethylammonium ion.

inactivation. I_{Na} and I_g in this figure are from an axon with only about half of inactivation still intact. The I_g trace is almost identical to that from the normal axon (left frame), and is not well reproduced by a single exponential (the smooth curve, fitted between the arrows).

To make a quantitative comparison of gating currents from normal and pronase-treated axons, the falling phase of I_g was fitted by the sum of two exponentials which were extrapolated to the beginning of the step (see Materials and Methods of preceding paper). The amplitudes (I_f, I_s) and time constants (τ_f^{ON}, τ_s^{ON}) of the components are given in Table II B. Also given is the ratio of steady-state to peak sodium current, which is an index of inactivation destruction (I_{ss}/I_p, where I_{ss} was measured 7 ms after the step). Pronase treatment to the degree shown does not selectively decrease the slow *ON* component or significantly alter its time constant. This result would be more satisfactory if a greater fraction of inactivation could be destroyed, but more severely treated axons usually have small currents and sloping base lines that make quantitation difficult.

The fast *ON* component of I_g seems clearly related to activation of the Na channels, although a successful model relating the two phenomena has not been devised. The slow *ON* component, on the other hand, does not correlate

with any previously described process. It is suggested below that each Na channel has open states, which we call x_1 and x_1y (in addition to state h_2 of Chandler and Meves, 1970; see preceding paper), and that the slow *ON* component is related to the transition from x_1 to x_1y.

No component of I_g, then, has the time course of inactivation, even during large depolarizations to +100 mV when inactivation has a rapid time course.

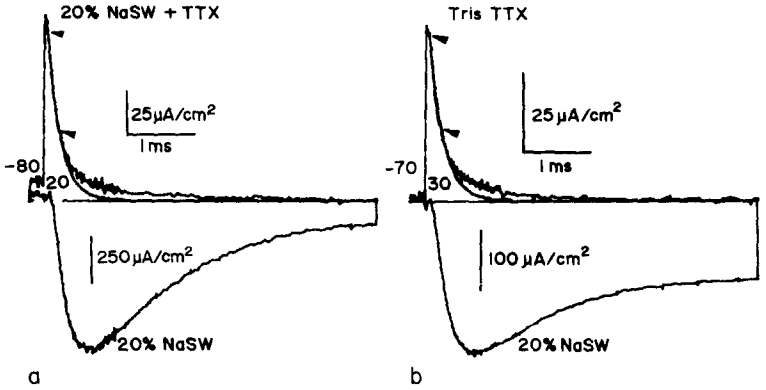

FIGURE 1. (*a*) I_{Na} inactivation and the slow *ON* component of I_g do not have the same time course. $I_{Na} + I_g$ was first recorded (not shown) in 20% Na SW. TTX was then added and I_g (upper trace) was recorded. I_g was then subtracted from $I_{Na} + I_g$ to yield I_{Na}, the lower trace. The smooth curve is an exponential fitted to I_g between the arrows. I_g has a distinct slow component that decays before inactivation is complete. 20% NaSW//190 TMA 10 Na, 8°C. Control pulses from −170 mV. (*b*) After removal of about one-half of inactivation by pronase treatment (different axon), the slow *ON* component is not noticeably affected. Smooth curve, an exponential fitted between the arrows, 20% Na SW and Tris TTX//200 TMA, 8°C. Control pulses from −120 mV.

Inactivation Immobilizes Two-Thirds of Gating Charge

Although no component of I_g seems directly associated with it, inactivation does have a strong effect on I_g, as illustrated in Fig. 2. In part (*a*) of Fig. 2 the upward trace is *ON* gating current during a 10-ms pulse to +50 mV; and the inward tails are *OFF* gating currents when the pulse is terminated after the given duration. For pulses longer than ~1 ms, the amplitude of *OFF* current diminishes slightly with the duration of the pulse and the area encompassed by the tails decreases substantially. This can be seen easily in part (*b*) of Fig. 2, where the tails after 0.3- and 10-ms pulses are superimposed.

To study quantitatively this effect, *ON* charge movement was determined by integrating to the point of interruption of the step, and divided into *OFF* area, obtained by integrating the tail. The *OFF:ON* ratio is near 1 for pulses of short duration, but decreases to about one-third for long pulses (Fig. 3; data from two experiments).

The decrease of the ratio follows the time course of inactivation, as shown in Fig. 4, where I_{Na} and the *OFF:ON* ratio are plotted on the same time axis, for a depolarization to $V_m = 0$. The right part of the figure is a semilog plot of the time-dependent portion of the ratio. It is clear that inactivation of I_{Na} and

TABLE II

A, TIME CONSTANTS OF INACTIVATION (τ_h) AND THE SLOW COMPONENT OF I_g *ON* (τ_s^{ON})

V_m	τ_h	τ_s^{ON}	n*
mV	*ms*	*ms*	
20	1.18–1.7	0.28–0.51	5
80	0.59–0.93	0.19–0.26	3

B, FAST AND SLOW COMPONENTS OF I_g *ON* WITH AND WITHOUT PRONASE‡

Exp.	Pronase	V_m	I_{ss}/I_p	I_f	τ_f^{ON}	I_s	τ_s^{ON}
		mV		*μA/cm²*	*ms*	*μA/cm²*	*ms*
AU055B	yes	30	0.52	68	0.121	16	0.646
AU065A	yes	30	0.49	64	0.132	17	0.689
SE135D	yes	40	0.70	42	0.143	8	1.07
SE135D	yes	60	0.70	61	0.092	12	0.538
SE135C	no	20	0.17	133	0.128	23	0.720
AU216A	no	50	–	80	0.079	14	0.471
SE016C	no	50	0.17	107	0.107	14	0.337
SE046A	no	60	–	92	0.093	12	0.370

* Number of experiments.

‡ For explanation of symbols, see text.

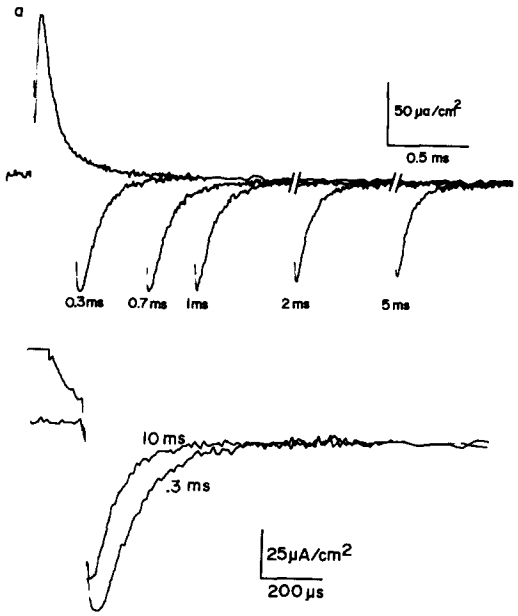

FIGURE 2. Immobilization of gating charge. (*a*) I_g was recorded with the P/4 method for a pulse from −70 to +50 mV. The inward tails were recorded on return to −70 mV after the indicated time at +50 mV. Control pulses started from −170 mV (−70 → +50 → −70, −170 → −140 → −170). The area encompassed by the tails decreases with pulse duration, as shown clearly in (*b*), where the 0.3- and the 10-ms tail are superimposed. The falling phase of *ON* current is seen in the 0.3 ms record. Tris SW + TTX//125 Cs, 8°C.

decrease of the *OFF:ON* ratio follow the same time course. The time constants for inactivation (τ_h) and decay of the time-dependent part of the *OFF:ON* ratio ($\tau_{OFF:ON}$) from this and other experiments are listed in Table V A. In all cases there is reasonable agreement between the two.

From the semilog plot in Fig. 4*b* it can be seen that decay of the *OFF:ON* ratio begins after a lag, as has been noted for the onset of Na inactivation (see preceding paper).

We interpret the decay of the *OFF:ON* ratio to mean that about two-thirds of gating charge is temporarily immobilized by inactivation, and returns to *off* position too slowly to be detected.

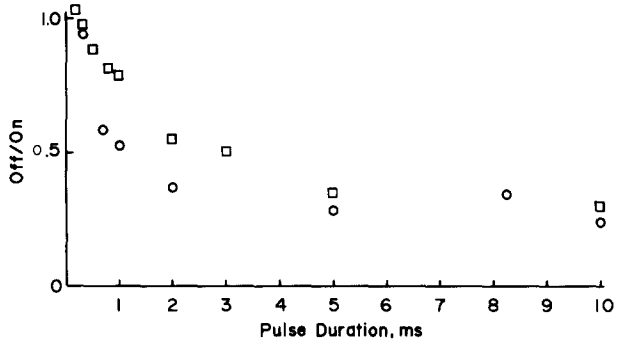

FIGURE 3. Immobilization of gating charge. *ON* is charge movement during a pulse to +10 (□) or +50 mV (○) and *OFF* is the inward charge movement on return to −70 mV. The *OFF:ON* ratio is near 1 for short pulses, and about one-third for long pulses. □, Tris SW + TTX//200 TMA. ○, Tris SW + TTX//125 Cs + 2 mM EDTA. 8°C. Control pulses started at −170 mV.

The V_m Dependences of Inactivation and Immobilization Are the Same

Inactivation of I_{Na} and I_g can also be demonstrated with the two-pulse experiment drawn in Fig. 5 (cf. Hodgkin and Huxley, 1952*a*). It is known that I_{Na} elicited by a second pulse is depressed for many milliseconds after the end of a prepulse. The effect of a prepulse on gating current is illustrated in Fig. 5, where the larger trace is the control (no P1) and the smaller is gating current during P2, which was applied 0.7 ms after termination of a 10-ms prepulse. The most obvious effect of the prepulse is a reduction of the total charge transferred during P2. About half of the charge is lost, presumably immobilized by inactivation. There is also a change in the time course of I_g, which has a faster rising phase and probably a disproportionately reduced slow *ON* component.

A two-pulse experiment can be used to determine the V_m dependence of charge immobilization, and thus to get something analogous to the h_∞ curve of Hodgkin and Huxley (1952*a*), by varying P1 while P2 is fixed. The voltage pattern and results are in Fig. 6 (*upper*). The circles represent peak I_{Na} in P2 plotted as a function of V_m during P1 (V_{P1}). I_{Na} has been normalized relative to I_{Na} with no prepulse ($V_{P1} = -70$ mV), and is given by the ordinate. The resulting curve falls to about 18% of control for V_{P1} about +10 mV, and its midpoint is

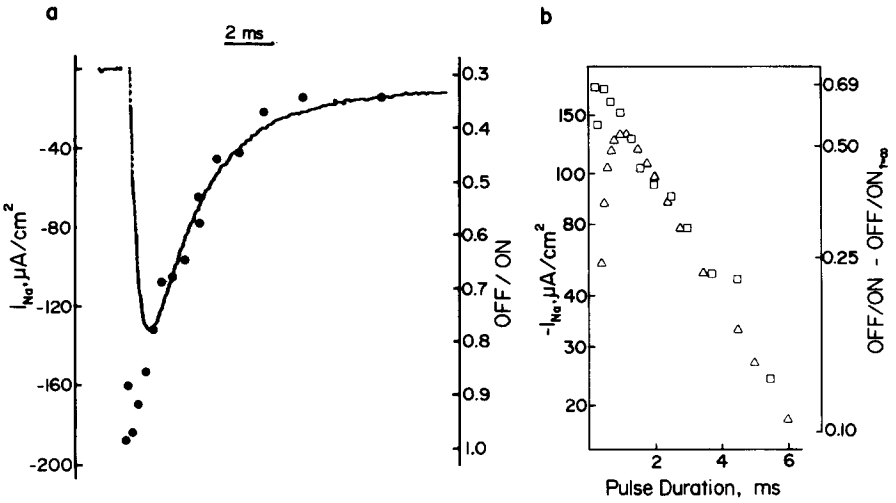

FIGURE 4. The time course of inactivation and charge immobilization are the same. (*a*) The experimental trace is I_{NA} for a depolarization from −70 to 0 mV. The dots give the *OFF:ON* ratio under the same conditions, but after addition of TTX. (*b*) A semilog plot of the same data. 40 Na 50 Ca Tris ± TTX//200 TMA. 8°C. Control pulses from −160 mV.

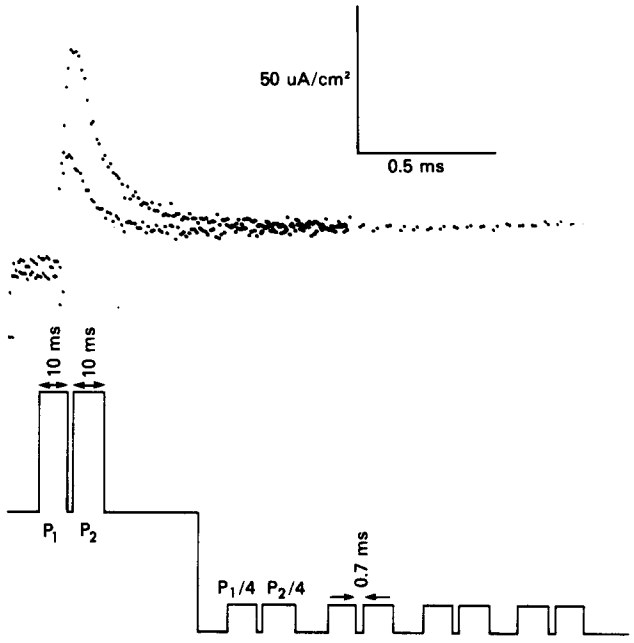

FIGURE 5. Charge immobilization resulting from inactivation by a prepulse. The lower amplitude trace is I_g for the pulse pattern shown in the *inset*. For the upper trace there was no prepulse. Tris SW + TTX//200 TMA, 8°C. Control pulses from −150 mV.

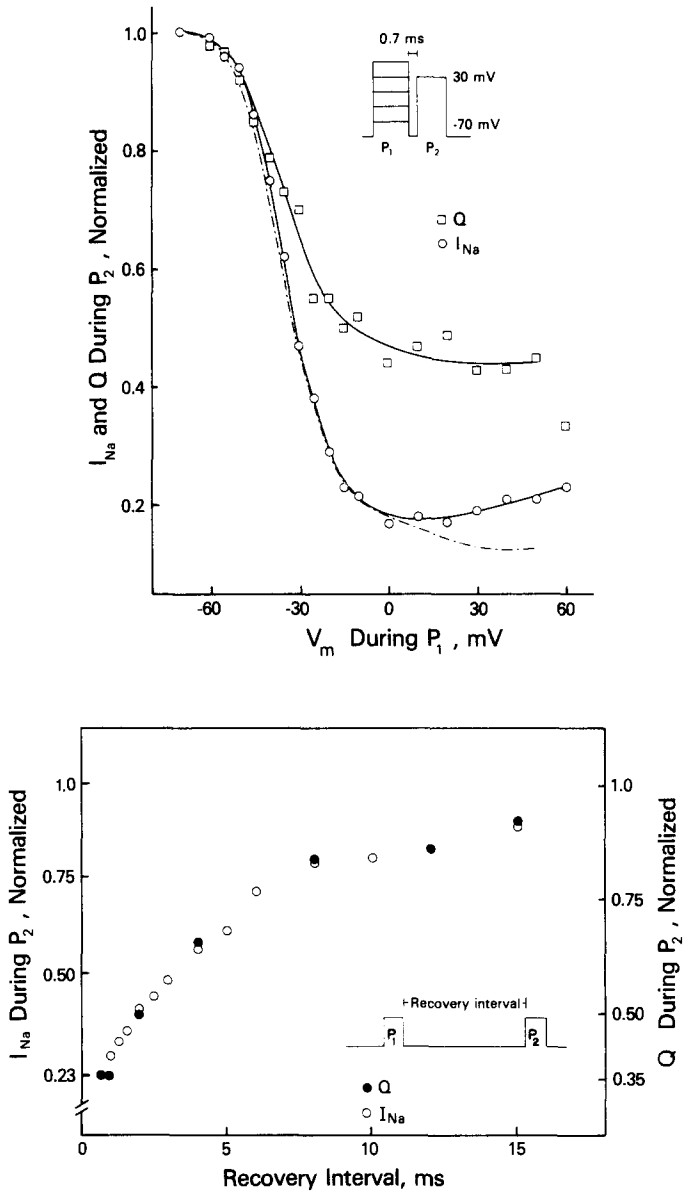

FIGURE 6. (*Upper*) The voltage dependence of inactivation and of charge immobilization is the same. The circles give I_{Na} during P_2 as a function of V_m during P_1 (see *inset*). The squares are gating charge (Q) movement during P_2. Curves through the points are drawn by eye, and the dashed curve is Q at expanded scale. 60 Na 50 Ca Tris ± TTX//200 TMA, 8°C. Control pulses from −170 mV. (*Lower*) Inactivation and charge movement (Q) recover with the same time course after a prepulse. Q is from one axon, I_{Na} from another. The abscissa is on a linear scale. Q, Tris TTX//200 TMA. Control pulses from −150 mV. I_{Na}, 60 Na 50 Ca Tris//200 TMA. Control pulses from −170 mV. 8°C.

about −35 mV. The midpoint is substantially to the right of that usually reported, perhaps because of our unusual ionic conditions. We have not explored this point.

Total Q movement during P2 was determined by integrating I_g traces recorded after adding TTX, and is given by the squares. The Q curve resembles that for I_{Na}, but its lowest value is about 44% of control; i.e. immobilization is less complete than Na inactivation. For closer comparison, the Q curve (drawn by eye) was scaled up to give the dashed line, which follows I_{Na} very closely except for a divergence for V_{P1} more positive than about +10 mV. The significance of the divergence is unknown, but over most of the voltage range inactivation and immobilization have the same voltage dependence.

Immobilized Charge Recovers together with Inactivation

Inactivated Na channels recover over the course of 30 ms or so at −70 mV, as can be shown by varying the interval between P1 and P2 (Fig. 6 *lower*). The open circles in the figure give peak I_{Na} in P2 normalized relative to the control value (no P1) and plotted as a function of the recovery interval. The filled circles are total Q in P2, taken from another experiment. Q has been normalized relative to the control value, and is measured by the right ordinate. For a recovery interval shorter than 0.7 ms neither I_{Na} nor I_g from P1 has subsided completely, making the curves hard to interpret. For this reason, the Q and I_{Na} curves have been scaled to coincide at 0.7 ms. For longer intervals they closely follow each other, again pointing to the conclusion that charge immobilization is the result of inactivation. Time constants for recovery of I_{Na} (τ_h) and of charge movement (τ_Q) for this and other experiments are listed in Table V B.

Rapid Recovery of Q Movement at −150 mV: the Slow OFF Component

In the preceding sections it has been shown that a fraction of gating charge is temporarily immobilized by inactivation of Na channels, and as a result returns to *off* position too slowly to detect with certainty when V_m is −70 mV. The recovery process for I_{Na} is a great deal faster at −150 mV, and has a time constant of about 0.6 ms at 8°C (see preceding paper and Table V B). If inactivation is preventing return of immobilized charge, then I_g at −150 mV should have a component with a time constant of about 0.6 ms, representing immobilized charge that is freed by recovery from inactivation.

I_g tails recorded at −150 mV after long depolarizing pulses do indeed have a component with the appropriate time constant, as seen in Fig. 7*a*. The voltage pattern is in the *inset*. After a pulse to +10 mV for 10 ms, which is long enough for inactivation to reach a steady level, I_g has a prominent slow component (called hereafter the slow *OFF* component) with a time constant of 0.7 ms, which is close to that for recovery from inactivation at −150 mV (Table V B). Time constants for the slow *OFF* component from several experiments are listed in Table V C under the heading τ_s^{OFF}, and they range from ~0.4 to 0.7 ms.

Inactivation does not occur significantly during a 0.7-ms pulse to +10 mV (Fig. 7*a*) and, as expected, I_g after this pulse decays approximately as a single exponential; there is no slow *OFF* component.

The slow *OFF* component is reduced by pronase which destroys inactivation, as illustrated in Fig. 7*b*. The traces are from an axon with only 30% of inactivation still intact. Tails after 0.7- and 10-ms pulses are quite similar to each other (compare with Fig. 7*a*) but the amplitude of the 10-ms tail is slightly reduced and it has a small slow *OFF* component that is presumably related to the intact portion of inactivation.

We interpret these results as meaning that charge immobilized by inactivation can move back to *off* position after recovery from inactivation; and at −150 mV this happens rapidly enough to produce the slow *OFF* component. Other possible contributions to this component are discussed below.

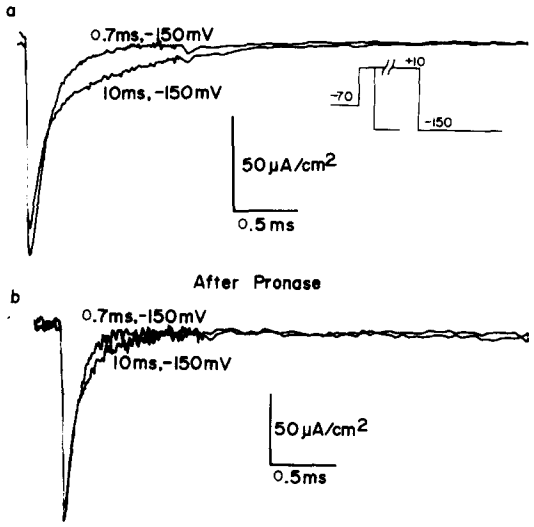

FIGURE 7. Slow *OFF* component at −150 mV. (*a*) The voltage sequence was −70 → +10 → −150 mV. The traces begin just before the step from +10 to −150 mV, after 0.7 or 10 ms at +10. The 10-ms tail has a prominent slow *OFF* component. 15% NaSW + TTX//125 TMA, 5°C. Control pulses from −170 mV. (*b*) The same procedure in another axon (but with the sequence −80 → +20 → −150), after pronase had destroyed 70% of inactivation. The slow *OFF* component is almost entirely gone. 90 Na 50 Ca 40 Mg + TTX//190 TMA 10 Na, 8°C. Control pulses from −130 mV.

The Slow Component of Tail I_g Develops with the Time Course of Inactivation

The slow *OFF* component of I_g described above is not present after a short depolarizing pulse, before inactivation occurs. To ascertain that it develops with the time course of inactivation, we fitted the tails after pulses of different durations with two exponentials, beginning about 50 or 60 μs after a step to −150 mV. Both exponentials were extrapolated to time zero (the beginning of the step to −150 mV) and Q movement associated with each component was taken as the product of the initial amplitude by the time constant. The extrapolation may well introduce some error, but it seems the only reasonable procedure if the current is to be separated into two components. The results are plotted as a function of pulse duration in Fig. 8. Charge movement in the fast component declines as slow *OFF* component charge increases, and the sum

of the two remains approximately constant. Both curves in Fig. 8 can be fitted with exponentials fairly well, and both have time constants of about 2.8 ms. For comparison, τ_h recorded from the same axon at the same voltage (0 mV) was 2.5 ms, which is in satisfactory agreement. Time constants for the growth of charge moving in the tail's slow *OFF* component (τ_1) and for the decline of charge movement in the fast component (τ_2) are listed in Table V C for several experiments. We conclude that these effects are a result of inactivation, and that the slow *OFF* component is (mainly) the charge immobilized by the inactivation process.

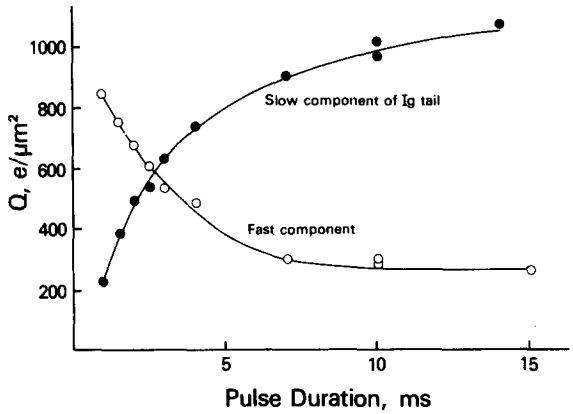

FIGURE 8. The slow *OFF* component at −150 mV develops with the time course of inactivation. The voltage sequence was −150 → 0 → −150 mV. I_g tails recorded on return to −150 mV were fitted with the sum of a fast and a slow exponential, and both exponentials were extrapolated to the beginning of the step back to −150 mV. The charge transferred in each component is plotted as a function of the interval at 0 mV. The decrease of the fast charge and the increase of the slow charge parallel the time course of inactivation. 40 Na 50 Ca Tris + TTX//200 TMA, 8°C. Control pulses from −160 mV.

OFF Charge Exceeds ON for Pulses from −140 or −150 mV

At −140 or −150 mV recovery from inactivation is so fast that the charge immobilized by inactivation can be seen as it returns to *off* position, and it constitutes or contributes to the distinct slow *OFF* component in Fig. 7*a*. In addition to immobilized charge, this component should also contain charge associated with the two gating processes that have time constants of about 0.5 ms at this voltage: inactivation, and closing of K channels. τ_h, a measure of inactivation and recovery kinetics, is approximately 0.5 ms at −140 mV compared to about 2.5 ms at 0 mV. I_K rises to 50% of its final level in 4.7 ms at 0 mV (8°C) and decays with a half-time of ~0.4 ms at −140 mV. As a result of faster kinetics, gating current associated with either process should be much easier to see at −140 mV than at 0 mV. It is therefore of interest to know if Q_{OFF} for pulses from −140 mV exceeds Q_{ON}, i.e. to see if some gating charge movement that escaped detection during depolarization is visible at −140 mV.

An experiment to test this point is shown in Fig. 9*a*. In this experiment V_m was stepped from −70 mV, the holding potential, to −140 mV 10 ms before

application of a pulse to 0 mV (−70 → −140 → 0 → −140 mV). Gating current during the pulse is similar to that in Fig. 2*a*, where the pulse rises from −70 rather than −140 mV. When the pulse is terminated after 0.5 ms (trace labeled 0.5) I_g *OFF* decays to a good approximation as a single exponential; but after a

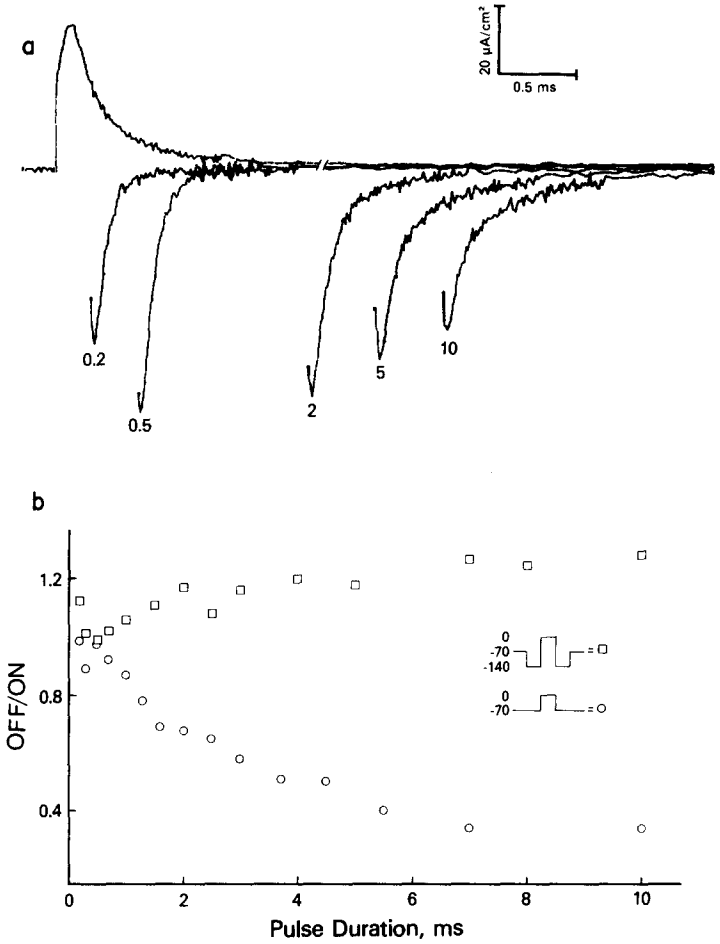

FIGURE 9. (*a*) Gating current and charge movement for pulses from −140 mV. The pulse sequence for the traces is given by the upper *inset* in part (*b*) of the figure. The numbers give the duration of the pulse to 0 mV. (*b*) *OFF:ON* ratios for pulses from −70 mV (circles) and −140 mV (squares). Total charge was determined by direct integration of the traces, with no extrapolation. At −70 mV charge immobilized by inactivation returns too slowly to detect, and *OFF:ON* drops to about one-third. At −140 mV *OFF* charge slightly exceeds *ON* for long pulses. 40 Na 50 Ca Tris + TTX//200 TMA, 8°C. Control pulses from −160 mV.

10-ms pulse initial amplitude is reduced and there is a prominent slow *OFF* component like that in Fig. 7*a*.

The ratios of *OFF* to *ON* charge movement for this experiment are presented in Fig. 9*b* for pulses rising either from −70 or −140 mV. Charge was

determined by direct integration of the traces, with no extrapolation. For pulses from −70 mV, *OFF:ON* is near 1 if the pulse is short, and about one-third if it is long (circles, Fig. 3). When the starting voltage is −140 mV the ratio is again approximately 1 for short pulses, but rises to about 1.2 for long ones. *OFF:ON* for a number of similar experiments is given in Table III, for a 10-ms pulse from −140 or −150 mV to the voltage listed. There is substantial variation in the ratio even for two similar determinations from one axon, and we have been unable to detect a consistent pattern in these variations. If all the values are averaged, *OFF* charge movement exceeds *ON* by 19%, with a standard deviation of 15%. The excess, if it exists, may be due (among other possibilities) to gating charge directly associated with inactivation or with closing of the K channels. This is discussed further below.

TABLE III

OFF:ON RATIOS AT VERY NEGATIVE VOLTAGES*

OFF:ON	V_m	V_m during pulse	Exp. no.
	mV	*mV*	
1.27	−150	30	AU015A
1.11	−150	10	Se135B
1.44	−150	30	AU146A
1.03	−140	50	AU146A
1.02	−140	20	AU146B
1.0	−140	50	AU176A
1.22	−140	50	AU216A
1.30	−140	0	Se036A
1.19	−140	20	Se056A
1.30	−140	20	Se056A

* Pulse duration in all cases was 10 ms.

Inactivation Alters the Q-V_m Distribution

Fig. 10*a* compares the Q-V_m distribution for initially resting membrane with that for membrane with most of its Na channels activated by a 0.6-ms pulse to +20 mV. The procedures are diagrammed in the *insets*. *ON* is the integral of current during a 10-ms pulse to the voltage on the abscissa, while *A* is integrated current during a second step, which was applied after 0.6 ms at +20 mV. Curves have been drawn through the points by eye, and for ease of comparison *A* (which stands for initially activated) has been translated along the vertical axis. From the similarity of the *ON* and the *A* curves it is clear that activation does not alter the Q-V_m distribution. Stated more precisely, activation does nothing to the distribution that cannot be reversed within a few milliseconds, the period of integration during the second pulse.

If the first pulse is long enough for inactivation to occur, the distribution does change, as shown by curve *I* in Fig. 10*b*, where the initial pulse was to −20 mV for 15 ms. Charge movement in the *I* curve (*I* stands for initially inactivated) between +20 and −70 mV is about one-third as large as in the *ON* curve, for which there was no inactivation. According to the explanation given above, inactivation has immobilized about two-thirds of the charge. For V_m negative to

−70 mV the *I* curve steepens, presumably because of the increased amplitude and faster time course of the slow *OFF* component. At −70 mV this component is too small to contribute significantly to integrated charge movement, but as voltage is made more negative its contribution becomes appreciable. Had the voltage range been extended to −150 mV, the *I* curve would probably have coincided with or even crossed below the *ON* curve (cf. Fig. 9, where the *OFF:ON* ratio exceeds 1 for long pulses).

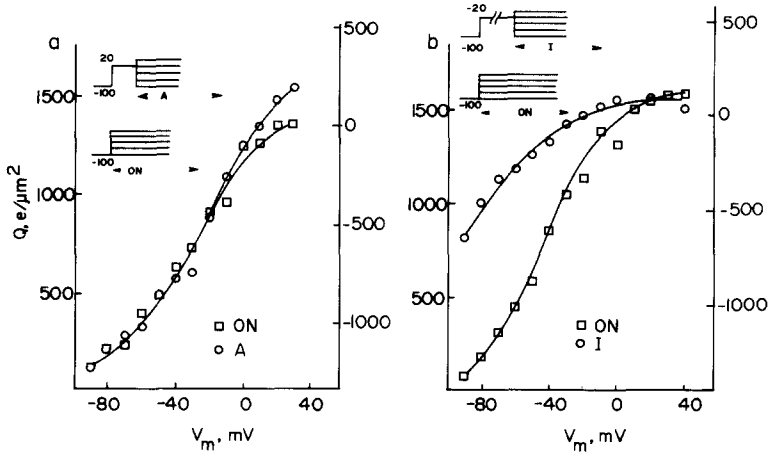

FIGURE 10. Activation does not alter the Q-V_m distribution, but inactivation does. (*a*) Na channels were activated by a 0.6-ms pulse to +20 mV, and the Q-V_m distribution at the end of this pulse was measured (curve *A*); i.e. each point on *A* is charge movement during a second pulse to the voltage on the abscissa. Curve *A* is not significantly different from the *ON* curve, which was determined in the usual way. *A* is measured by the right ordinate, *ON* by the left. Tris SW + TTX//200 TMA, 8°C. (*b*) After 15 ms at −20 mV, inactivation has occurred and the Q-V_m distribution in the second pulse (curve *I*) no longer resembles *ON*. Tris SW + TTX//125 Cs. 8°C. Parts (*a*) and (*b*) are from different axons.

Inactivation of I_g Demonstrated by Other Procedures

Immobilization of gating charge can also be demonstrated with the holding potential ±T method (see Armstrong and Bezanilla, 1974); i.e. −70 → −70 + T, with control pulse −70 → −70 − T. In this case interpretation is difficult because there can be substantial nonlinear current flow during the control pulse to −70 − T mV. The voltage patterns used in the experiment are in parts ii*a* and ii*b* of Fig. 11, and T was 80 mV. In Fig. 11*a*, a prepulse does (*P*) or does not (*N*) precede the +T pulse, but there is never a prepulse before −T. Both I_{Na} and I_g are depressed by a prepulse (traces in i*a*), and the effect on I_{Na} is more pronounced.

Summing current from positive and negative pulses is necessary to eliminate the linear part of capacitative current, so each of the traces in i*a* is the sum of current during +T and −T pulses. Attempts to reconstruct current during the individual pulses is given by iii for +T and by iv for −T. As reconstructed, I_g is depressed less than I_{Na} in iii*a* P because I_g inactivates less completely. The −T

pulse was not preceded by a prepulse in part (*a*) of the figure, so the *N* and *P* traces in iv*a* are identical (see description below). These theoretical traces sum to give the experimental record, i*a*. That is, i*aN* = iii*aN* + iv*aN*, and i*aP* = iii*aP* + *iv aP*.

In part (*b*) of the figure the situation is reversed: a prepulse does (*P*) or does not (*N*) precede the −T pulse, and there is never a prepulse before +T (see ii*b*). The prepulse in this case decreases I_g without altering I_{Na} (i*a*). In the

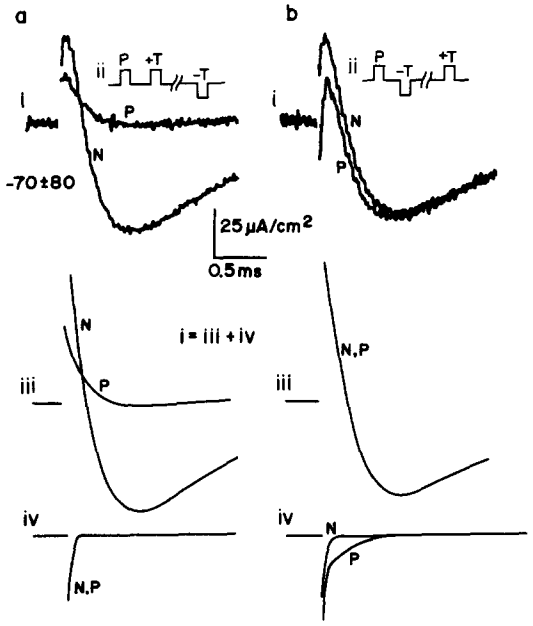

FIGURE 11. Inactivation of I_g produced by other pulse patterns. *ia* and *b* are experimental records of I_{Na} + I_g averaged from 20 repetitions of the pulse sequences in *ii a* and *b*, with (*P*) and without (*N*) a prepulse (pulse *P*). The current traces in *ia* and *b* begin just before the ±T pulses, and give the sum of membrane current in +T and −T. *iii a* and *b* are hypothetical reconstructions of current during +T with and without prepulse, and *iv a* and *b* are the same for −T.

reconstruction the current during +T is the same for both *N* and *P* for there was no prepulse before +T in either case. During the −T pulse there is a quickly decaying inward current in the absence of a prepulse (iv*bN*, and also iv*aN* and *P*). This current has been postulated to sum with outward gating current during the +T pulse to yield a trace that has an initial rising phase, the usual pattern for I_g recorded with the −70 ± T method (Armstrong and Bezanilla, 1974). When there is a prepulse (ivbP), the current has in addition a slow *OFF* component, for V_m is −150 mV and most of the Na channels are still inactivated as a result of the prepulse. As in Figs. 7 and 9 the slow *OFF* component is caused by the return to *off* position of charge immobilized by inactivation. The traces of iii*b* and iv*b* sum to give the experimental traces in i*b*.

When the voltage pattern is such that a prepulse precedes both +T and −T, the result is almost complete suppression of I_g as well as I_{Na} (not illustrated

here, but see Bezanilla and Armstrong, 1974; 1975*a*). This result can be reconstructed by summing trace iii*aP* (prepulse before +T) with trace iv*bP* (prepulse before −T).

The results of this section are completely consistent with those described in earlier sections.

Na Channels May Have Three Open States

In the preceding paper evidence was presented for two open states of a sodium channel. One is the state here called x_1, which derives from the Hodgkin and Huxley formulation (1952*a*), and the other is state h_2 of Chandler and Meves (1970). There is evidence in the literature for yet another open state. It has been noted that for brief depolarizations, before significant inactivation occurs, the time course of decay of I_{Na} tails on repolarization increases with the duration of the depolarizing pulse (Frankenhaeuser and Hodgkin, 1956; Chandler and Meves, 1970). This result implies the existence of an open state called x_1y here, which is occupied in the same voltage range as state x_1, but is distinguished from x_1 by its slower closing kinetics.

We have repeated this experiment, i.e. measuring decay rates of current tails after pulses of different length, and a typical result is given in Table IV. To avoid series resistance problems, the axon was in 15% NaSW (with 125 mM CsF inside), and there was compensation for 4 Ωcm^2 of series resistance. For a depolarization to +10 mV with return to −70 mV, the time constant of decline of I_{Na} increased from 135 μs to 175 μs as pulse duration increased from 0.3 to 1 ms, and the time constant of I_g (τ_{I_g}) increased from 146 to 216 μs. For larger depolarizations, the maximum value of the time constants is the same (about 175 and 204 μs) but these values are attained with shorter pulses: the underlying changes occur more quickly.

In the Discussion these findings are taken as evidence for the existence of the open states x_1 and x_1y, and for a voltage-dependent rate of transition from one to the other. The postulated relation between x_1, x_1y, and h_2 is shown in Fig. 12.

DISCUSSION

The major finding of this paper is that a large fraction of gating charge is immobilized as a result of inactivation of Na channels. If inactivation were complete (in Fig. 6*a*, for example, 20% of G_{Na} does not inactivate), only about one-fourth of gating charge would remain free to move. The immobilized charge returns to *off* position with the time course of recovery from inactivation (Fig. 6*b*) too slowly to be detected at −70 mV, but rapidly enough to be easily detectable at −150 mV.

A number of correlations between inactivation and charge immobilization are given in Table V. In most experiments, (*a*) the time constants of charge immobilization and inactivation agree closely (Table V A; Fig. 4), as do (*b*) the time constants of recovery of charge movement and recovery from inactivation (Table V B; Fig. 6*b*). (*c*) The slow *OFF* component of gating current in tails recorded at −140 or −150 mV (Fig. 7*a* and 9*a*) has approximately the same time constant as recovery from inactivation at similar voltages (τ_s^{OFF}, Table V C

vs. τ_h, Table V B). (*d*) Finally, total charge movement in the slow *OFF* component of I_g tails grows with a time constant (τ_1, Table V C; Fig. 8) that is close to τ_h at similar voltages (Table V A); and the fast component charge movement of tails decreases with about the same time constant (τ_2, Table V C). That is, immobilized charge as expressed by the total charge in the slow *OFF* component grows with the time constant of inactivation, to a good approximation. All of these correlations show that charge immobilization and inactivation are manifestations of the same phenomenon. Meves and Vogel (1977) have recently described similar findings, but they report that a somewhat smaller fraction of total charge is immobilized, and that the time courses of inactivation and charge immobilization do not agree closely in all cases.

TABLE IV

DECAY TIME CONSTANTS FOR I_{Na} AND I_g AT −70 mV

V_m during pulse	Pulse duration	$\tau_{I_{Na}}$	τ_{I_g}
mV	*ms*	*μs*	*μs*
+10	0.3	135	146
+10	0.7	165	204
+10	1	175	216
+50	0.3	155	194
+50	0.7	171	224
+50	1	171	206

We have found no charge movement in the *ON* transient that seems directly associated with inactivation. The fast *ON* component is almost certainly related to activation of G_{Na}, but the slow *ON* component does not correlate with any known process. If the falling phase of *ON* current is fitted with the sum of two exponentials and both are extrapolated to time zero, the fast component accounts for more than half of the total charge movement. Since two-thirds of the total charge can be immobilized, it seems clear that inactivation must immobilize some charge that is, on kinetic grounds, most reasonably linked to activation. This suggests that activation and inactivation are coupled in some way, and are not the independent gating factors described by the Hodgkin and Huxley equations.

Before proceeding it is worthwhile to list the various current components we have seen and summarize information about them. (*a*) The fast *ON* component is probably related to Na activation but a precise model is lacking. This component is reduced by inactivation. (*b*) The slow *ON* component is reduced by inactivation, perhaps more strongly than the fast component. It is unaffected by pronase, as best we can tell (Fig. 1*b*; Table II *b*). A possible origin of this component is given in the model of Fig. 12. (*c*) The charge that is not immobilized by inactivation forms the fast *OFF* component of the tail at −150 mV. This component is presumably related to the activation gating structures, but it is not known precisely how. (*d*) The charge that is immobilized by inactivation forms (or is the major part of) the slow *OFF* component of the tail at −150 mV. The model in Fig. 12 provides an explanation of charge immobilization. (*e*) The final component is the "excess" *OFF* charge at −150 mV after a

long depolarization, i.e. the excess of *OFF* over *ON* charge (Fig. 9*b*; Table III). The kinetics of this excess charge movement are not clear, but it may contribute to the slow *OFF* component. The origin of the excess charge has not been demonstrated, but for the following reasons we think it is associated with gating of the K channels. If this charge moves in the slow component, as seems likely, its kinetics are appropriate either to opening of the Na inactivation gates

TABLE V

CORRELATIONS BETWEEN Na INACTIVATION AND Q_g IMMOBILIZATION

A.	V_m	τ_h	$\tau_{OFF:ON}$	Exp.
	mV	*ms*	*ms*	
	−10	3.1	3.2	AU276C
	+10	1.6	1.2	"
	0	2.3	1.8	SE016C
	+10	1.9	2.3	"
	0	2.4	2.5	SE036A
	+40	1.1	1.0	"
	+20	–	2.4	SE056A
	+10	–	1.3	SE135D

B.	V_m during recovery	τ_h	τ_Q	Exp.
	mV	*ms*	*ms*	
	−70	2.9	–	JL235B
	−130	0.6	–	"
	−60	6.2	7.7	SE135C
	−70	6.0	5.5	"
	−150	0.55	0.57	"
	−70	–	5.2	AU216A
	−140	–	0.6	"
	−70	11.9	6.3	AU266A
	−100	2.7	2.4	"
	−70	6.6	6.5	Se106A
	−100	2.0	1.8	"
	−70	8.2	8.3	Se036B
	−100	2.3	2.3	"
	−70	5.9	4.5	Se096D

C.	V_m	V_{pulse}*	τ_s^{OFF}‡	τ_1	τ_2	Temperature	Exp.
	mV	*mV*	*ms*	*ms*	*ms*	*°C*	
	−140	0	0.64	2.8	2.7	8	Se036A
	−150	+30	0.43	1.4	1.9	8	AU015A
	−150	+30	0.39	1.6	1.2	8	AU146A
	−140	+50	0.42	<1.5	<1	5	AU176A
	−140	+50	0.52	1.1	0.8	8	AU216A
	−150	+20	0.7	–	–	5	JL215A

A, Time constants of inactivation (τ_h) and decay of the *OFF:ON* ratio ($\tau_{OFF:ON}$), 8°C.

B, Time constants of recovery from inactivation (τ_h) and of Q (τ_Q), 8°C.

C, Time constant of slow component of tail: τ_s^{OFF}. Time constant of growth of Q in slow component of tail: τ_1. Time constant of diminution of Q in fast component of tail: τ_2. The tail of I_g, recorded at V_m, was fitted with two exponentials as described in the text. Total charge in the slow component grew as a function of pulse duration, with time constant τ_1. Total charge in the fast component decreased with time constant τ_2.

* Tails were recorded at V_m, after a pulse to V_{pulse}.

‡ Determined at the end of a 10-ms pulse.

or to closing of the K channel gates. It must be admitted at the outset that there is little evidence on which to base a judgement. Both gating processes have slow kinetics during depolarization and are expected to produce small, slowly changing currents that might be overlooked. During very large depolari-

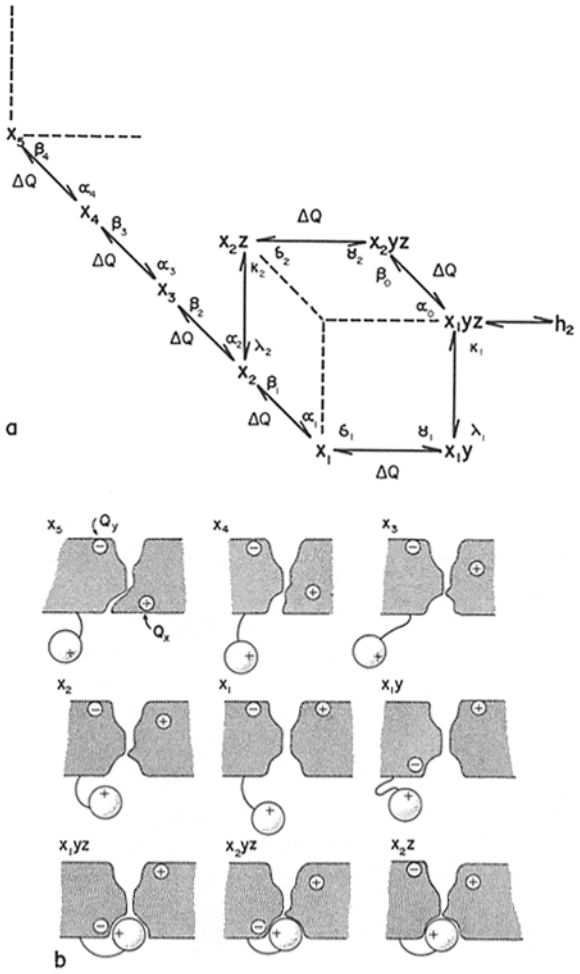

FIGURE 12. A state diagram of an Na channel, and its mechanical representation. See text. State h_2 has been omitted from the mechanical model.

zations, however, τ_h drops to approximately 0.5 ms, which is near its value at −150 mV. Nonetheless, even for a large depolarization there is no suggestion of a gating current component with time constant similar to inactivation, leading us to postulate that there is no charge movement directly associated with this process. This is theoretically plausible, as shown below, and in the preceding paper. On the other hand, gating current associated with the K channels is a theoretical necessity, if these channels are independent of the Na channels as all the evidence indicates (see, for example, Hille, 1970; Armstrong, 1975).

A Model for Na Inactivation

The state diagram of Figure 12 and its mechanical representation are an attempt to account for the data both of this paper and of the preceding one (Benzanilla and Armstrong, 1977 a). The major points we have sought to explain both in this paper and the proceeding one are: (*a*) Na activation and inactivation are coupled, not independent; (*b*) there is little or no charge movement directly associated with inactivation; (*c*) approximately two-thirds of gating charge is immobilized by inactivation; and (*d*) there are at least three open states of an Na channel.

In the figure, a sodium channel is imagined to have four "closed" states (x_5, x_4, x_3, x_2), three open states (x_1, x_1y, h_2), and three inactivated states (x_1yz, x_2yz, x_2z). The conductance of a closed or inactivated channel is zero, while the conductance of states x_1, x_1y, and h_2 is about 10^{-11}S per channel. Permissible transitions among the states are indicated by arrows, and those with voltage-dependent equilibrium constants are marked by the symbol ΔQ, which means that charge movement occurs during the transition. Steps along the x axis signify changes in the activation gating structure, and generate the fast component of *ON* gating current. In the mechanical representation fast I_g is generated by the movement of Q_x, which causes, in some unspecified way, the conformational changes seen in the drawings of states x_5–x_1. Q_x could equally well be negative and moving in the opposite direction.

Gating current associated with steps along the y axis is relatively slow. This axis represents the position of a hypothetical charge (Q_y) that makes the channel mouth either attractive to the inactivating particle ($y = 1$, states x_1y, x_1yz, and x_2yz) or unattractive ($y = 0$). In the mechanical representation, charge Q_y is near the channel mouth when $y = 1$, and it electrostatically attracts the oppositely charged inactivating particle. The attraction is mutual, and Q_y is stabilized in its position near the channel mouth when the inactivating particle is blocking the channel.

Steps along the z axis correspond to movement of the inactivating particle in and out of the channel mouth. Although the particle is charged, there is little or no gating current associated with these steps, for the particle does not move a significant distance through the membrane field. In state x_2yz and x_2z the channel is blocked by the inactivating particle, and the activation gate is partially closed. x_2yz is relatively stable because Q_y attracts the inactivating particle, but x_2z is unstable and decays quickly to x_2.

During opening and inactivation of a channel the most probable path is

$$x_5 \text{ or } x_4 \xrightarrow[\text{(fast } ON\text{)}]{\Delta Q} x_1 \xrightarrow[\text{(slow } ON\text{)}]{\Delta Q} x_1y \rightarrow x_1yz.$$

Conductance rises with a sigmoid time course because a channel must pass through several closed states before reaching the first open one (x_1).

During recovery from inactivation the most probable path is

$$x_1yz \xrightarrow[\text{(fast } OFF\text{)}]{\Delta Q} x_2yz \xrightarrow[\text{(slow } OFF\text{)}]{\Delta Q} x_2z \rightarrow x_2 \xrightarrow[\text{(slow } OFF\text{)}]{\Delta Q} x_4 \text{ or } x_5.$$

The rate-limiting step is $x_2yz \rightarrow x_2z$, a voltage-dependent transition that governs the rate of recovery. Charge that is not immobilized by inactivation moves during the step $x_1yz \rightarrow x_2yz$.

Closing of the channels after a brief pulse during which there is no significant inactivation follows the path

$$x_1y \xrightarrow{\Delta Q} x_1 \xrightarrow{\Delta Q} x_4 \text{ or } x_5.$$

The *OFF* charge movement associated with these steps (e.g., the 0.3 ms trace in Fig. 2*a*) has not been given a name. It is rapid, but quite distinct from the fast *OFF* component which is seen only after steps of long duration.

The model accounts for various experimental findings as follows.

(*a*) DELAYED ONSET OF INACTIVATION After depolarization a typical channel progresses from state x_5 or x_4 to x_1yz. Inactivation ($x_1y \rightarrow x_1yz$) cannot occur until the preceding steps are completed, and its onset is thus delayed.

(*b*) SLOW INACTIVATION FOR SMALL DEPOLARIZATIONS Inactivation is very slow whenever the rate constants β_i are large enough to cause significant retention of channels in the closed states. At all voltages calculation shows that τ_c and τ_h (see preceding paper) are equal for this model, as they are for the simpler model of the preceding paper.

(*c*) V_m-DEPENDENT INACTIVATION Inactivation after depolarization derives its voltage dependence from the preceding steps $x_5 \dashrightarrow x_1y$. $x_1y \rightarrow x_1yz$ is the slowest step and does not involve charge movement, so no gating current component has the time course of inactivation. During recovery the rate-limiting step is $x_2yz \rightarrow x_2z$, a transition that is voltage dependent.

(*d*) PRONASE EFFECTS Pronase prevents the steps $x_1y \rightarrow x_1yz$ and thus removes inactivation. It does not affect $x_1 \rightarrow x_1y$, and the slow *ON* component of gating current which is generated by this step is unchanged by pronase (Fig. 1*b*; Table II *b*).

(*e*) CHARGE IMMOBILIZATION During recovery from inactivation at −70 mV the step $x_2yz \rightarrow x_2z$ is very slow. The charge movement associated with this step and the subsequent ones ($x_2 \dashrightarrow x_5$) is thus spread out in time, and generates a current that is lost in the base-line noise. At −150 mV this step is faster but still rate limiting and it determines the time course of the slow *OFF* component, which is composed of charge movement associated with steps $x_2yz \rightarrow x_2z$ and $x_2 \dashrightarrow x_4$ or x_5.

(*f*) CHARGE THAT IS NOT IMMOBILIZED BY INACTIVATION This charge is associated with step $x_1yz \rightarrow x_2yz$. Functionally, this step serves to close the channel so that it does not leak during recovery from inactivation as it would if the recovery path were by way of a conducting state (x_1 or x_1y).

(*g*) VARIATION OF CLOSING KINETICS WITH PULSE DURATION For a very brief depolarization, some channels reach state x_1, but very few progress further and closing from this state is rapid. For a somewhat longer depolarization (0.7 or 1 ms) many channels reach state x_1y, and closing is slower since the channels must pass through state x_1 in the process. Closing time course from state x_1y should be slightly sigmoid, and this is usually observed, though it is close to the limits of time resolution and is consequently hard to interpret.

No mechanical representation of state h_2 is given in Fig. 12, but it is easy to imagine an appropriate one. Q_y, for example, might have a third position still closer to the inner edge of the membrane, and in this position it might not effectively stabilize the inactivating particle in the channel mouth. Step $x_1yz \rightarrow h_2$ is not very voltage dependent and should make only a minor contribution to gating charge movement. This contribution has simply been ignored.

Microscopic Reversibility

A state diagram with a circular pathway, e.g.,

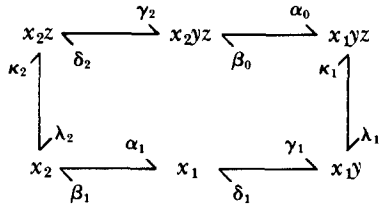

must meet the condition of microscopic reversibility if, as we postulate, there is no source of metabolic energy to fuel endless circulation around the loop. Compliance with this condition requires that for each step the forward flux be equal to the back flux, and from this it follows that

$$\alpha_1 \cdot \gamma_1 \cdot \kappa_1 \cdot \beta_0 \cdot \delta_2 \cdot \lambda_2 = \kappa_2 \cdot \gamma_2 \cdot \alpha_0 \cdot \lambda_1 \cdot \delta_1 \cdot \beta_1,$$

if there is microscopic reversibility. That is, the product of the rate constants going counterclockwise around the loop must equal the product of those going clockwise. Preliminary estimates indicate that sets of values for the constants can be found that are experimentally reasonable and comply with this condition. At present there are so many free parameters that explicit calculations do not seem worthwhile.

"Inactivation" in Pharmacological Studies

This model derives considerable support and inspiration from studies of pharamcological agents that block Na and K channels. Derivatives of TEA cause "inactivation" of K channels and it is clear that the channel must open before a derivative ion can assume its blocking position (Armstrong, 1971). Inactivation of Na channels can be destroyed by pronase, and a semblance of inactivation can then be restored by pancuronium (Yeh and Narahashi, 1975) or TEA derivatives (Rojas and Rudy, 1976). In myelinated fibers, strychnine causes something resembling inactivation, but with a more rapid time course (Shapiro, 1975). These compounds probably interact with Na channels in much the same way that TEA derivatives block K channels: they act from inside, and block channels that have open activation gates.

Noise Predictions

The model presented here makes a prediction regarding current fluctuations, or noise, which is quite distinct from the Hodgkin and Huxley predictions.

Specifically, in their model the inactivation gates open and close with a time constant τ_h, which is about 8 ms at −40 mV (8°C). This leads to the prediction of a corner frequency in the power spectrum of Na channel noise at the corresponding frequency, 19.9 Hz. In the present model, inactivation gates open and close with a time constant of $1/(\kappa_1 + \lambda_1)$, and τ_h, which is much larger, is not the time constant of a single process but instead reflects both activation and inactivation kinetics. $1/(\kappa_1 + \lambda_1)$ is roughly 0.5–1 ms, corresponding to a frequency of 160–320 Hz. The precise form of the predicted spectrum has not been worked out, but it seems clear that the corner frequency corresponding to inactivation is significantly higher than and perhaps testably different from the Hodgkin and Huxley predictions.

We are grateful to Dr. Michael Cahalan for much useful discussion, particularly with regard to current fluctuations. Drs. Meves and Vogel were very kind in letting us read their manuscript in advance of publication.

This work was supported by United States Public Health Service grant no. NS08951.

Received for publication 18 July 1977.

REFERENCES

ARMSTRONG, C. M. 1971. Interaction of tetraethylammonium ion derivatives with the potassium channels of giant axons. *J. Gen. Physiol.* **58**:413–437.

ARMSTRONG, C. M. 1975. Ionic pores, gates, and gating currents. *Q. Rev. Biophys.* **7**:179–210.

ARMSTRONG, C. M., and F. BEZANILLA. 1974. Charge movement associated with the opening and closing of the activation gates of the Na channels. *J. Gen. Physiol.* **63**:533–552.

ARMSTRONG, C. M., and F. BEZANILLA. 1975. Currents associated with the ionic gating structures in nerve membrane. *Ann. N. Y. Acad. Sci.* **264**:265–277.

ARMSTRONG, C. M., and F. BEZANILLA. 1976. A slow gating current component during recovery from inactivation. *Biophys. J.* **16**:27a.

BEZANILLA, F., and C. M. ARMSTRONG. 1974. Gating currents of the sodium channels: three ways to block them. *Science (Wash. D. C.).* **183**:753–754.

BEZANILLA, F., and C. M. ARMSTRONG. 1975*a*. Kinetic properties and inactivation of the currents of sodium channels in squid axons. *Philos. Trans. R. Soc. Lond.* Ser. B *Biol. Sci.* **270**:449–458.

BEZANILLA, F., and C. M. ARMSTRONG. 1975*b*. Properties of the sodium channel gating current. *Cold Spring Harbor Symp. Quant. Biol.* **XL**:297–304.

BEZANILLA, F., and C. M. ARMSTRONG. 1975*c*. Inactivation of gating charge movement. *Biophys. J.* **15**(2, Pt. 2):163*a*. (Abstr.).

CHANDLER, W. K., and H. MEVES. 1970. Evidence for two types of sodium conductance in axons perfused with sodium fluoride solution. *J. Physiol. (Lond.).* **211**:653–678.

FRANKENHAEUSER, B., and A. L. HODGKIN. 1957. The action of calcium on the electrical properties of squid axons. *J. Physiol. (Lond.).* **137**:218–244.

HILLE, B. 1970. Ionic channels in nerve membrane. *Prog. Biophys.* **21**:1–32.

HODGKIN, A. L., and A. F. HUXLEY. 1952*a*. The dual effect of membrane potential on sodium conductance in the giant axon of *Loligo*. *J. Physiol. (Lond.).* **116**:497–506.

HODGKIN, A. L., and A. F. HUXLEY. 1952*b*. A quantitative description of membrane

current and its application to conduction and excitation in nerve. *J. Physiol.* (*Lond.*). **117**:500–544.

KEYNES, R. D., and E. ROJAS. 1974. Kinetics and steady-state properties of the charged system controlling sodium conductance in the squid giant axon. *J. Physiol.* (*Lond.*). **239**:393–434.

MEVES, H. 1974. The effect of holding potential on the asymmetry currents in squid giant axons. *J. Physiol.* (*Lond.*). **243**:847–867.

MEVES, H., and W. VOGEL. 1977. Inactivation of the asymmetrical displacement current in giant axons of *Loligo forbesi*. *J. Physiol.* (*Lond.*). In press.

ROJAS, E., and B. RUDY. 1976. Destruction of the sodium conductance inactivation by a specific protease in perfused nerve fibers from *Loligo*. *J. Physiol.* (*Lond.*). **262**:501–531.

SHAPIRO, B. I. 1975. Block of ionic channels in axons by strychnine. *Biophys. J.* 15(2, Pt. 2):262*a*. (Abstr.).

YEH, J. Z., and T. NARAHASHI. 1975. Modification of sodium conductance kinetics of squid axon membranes by pancuronium. *Biophys. J.* **15**(2, Pt. 2):263*a*. (Abstr.).